Pergamon

Planet. Space Sci., Vol. 44, No. 9, pp. 917–925, 1996

0032–0633/96 $15.00+0.00

0032–0633(95)00133–6

Measurements of restitution coefficients of ice at low temperatures

M. Higa, M. Arakawa and N. Maeno

Institute of Low Temperature Science, Hokkaido University, Kita-ku Kita-19 Nishi-8, Sapporo 060, Japan

Received 5 May 1995; revised 6 October 1995; accepted 6 October 1995

Abstract. Measurements of the restitution coefficient (ε) of a smooth water ice sphere (radius = 1.5 cm) are made in a wide range of impact velocities ($1 \lesssim v_i \lesssim 700\,\mathrm{cm\,s^{-1}}$) and temperatures ($113 \lesssim T \lesssim 269\,\mathrm{K}$). The impact velocity dependence of ε is different in the quasi-elastic and inelastic regimes separated by a critical velocity (v_c) at which fracture deformation occurs at the impact point of ice samples. In the quasi-elastic regime ($v_i \lesssim v_c$), the value of ε is almost constant (0.88) and ice samples show no fracture deformations. In the inelastic regime ($v_i > v_c$), ε decreases with increasing v_i and ice samples have fracture patterns. The velocity dependence of ε is fitted as $\varepsilon(v_i) = (v_i/v_c)^{-\log_{10}e^{0.5}}$. v_c is shown to increase with decreasing temperature from 25 cm s^{-1} (269 K) to 180 cm s^{-1} (113–215 K).

Introduction

Saturn's rings consist of H_2O ice particles which collide with each other in a rotating disk. The collision phenomena among ice particles are the most important physical process to control the evolution of rings represented by a size distribution of particles (Greenberg *et al.*, 1977) and a macroscopic structure (e.g. Goldreich and Tremaine, 1978; Ohtsuki, 1992). To clarify the evolution of those physical properties, we need to understand the collision properties of ice particles and derive quantitative results on the coagulation, rebound and fragmentation phenomena in the environment of Saturn's rings.

The rebound process is described by the restitution coefficient (ε) which is defined as the ratio of the rebound velocity to the impact velocity. Measurements of ε in normal collisions between an ice sphere and ice block at low temperatures were made by Bridges *et al.* (1984) and Hatzes *et al.* (1988) (see Fig. 1), in order to understand the dynamical processes occurring in Saturn's rings. In their experiments, the impact velocity was controlled in a range lower than a few cm s^{-1} corresponding to the random velocity ($\lesssim 1\,\mathrm{cm\,s^{-1}}$) of the present rings of Saturn (Esposito, 1986). However, to study the origin and dynamic evolution of ring systems, we also require collisional properties of ice in a much wider velocity range. Furthermore, in their experiments, they used a compound disc pendulum system to achieve very low velocities. In this system the ice sphere has a moment of inertia with that of a pendulum added so that this collision might be different from actual sphere collisions as suggested by Dilley (1993). In order to extrapolate their useful data to actual sphere collisions in Saturn's rings, comparison of their data with those of actual sphere collisions is important.

Our experiment was initiated to measure systematically the restitution coefficient of an ice sphere (radius 1.5 cm) in a wide range of impact velocities (1–700 cm s^{-1}) and temperatures (269–113 K) as shown in Fig. 1. A preliminary report was made in Higa *et al.* (1993) and this paper is the second report of our experiment, which gives

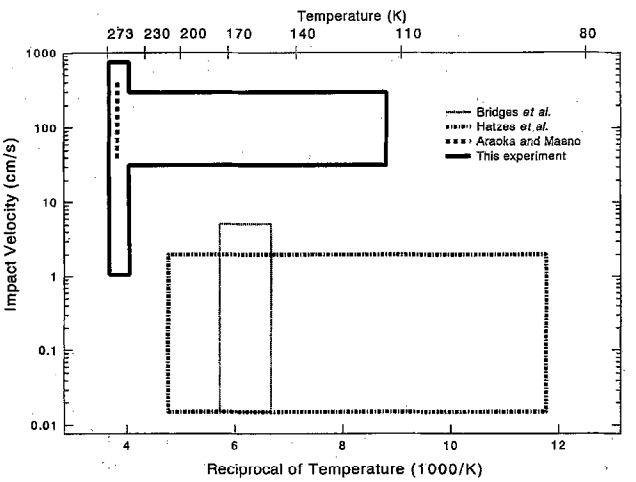

Fig. 1. Impact velocity and temperature regions, in which restitution experiments of ice were conducted

Correspondence to: M. Higa

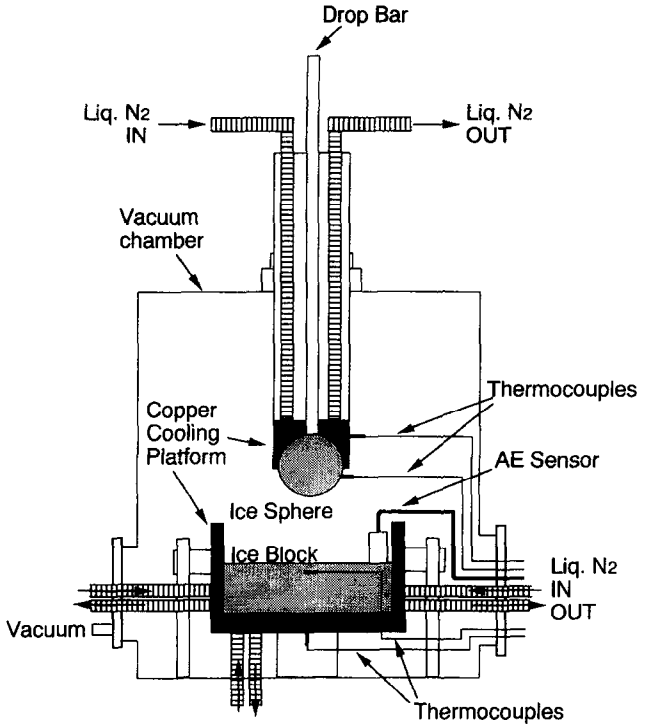

Fig. 2. Schematic picture of experimental apparatus

more detailed results of impact velocity and temperature dependence of the restitution coefficient of ice spheres.

Experimental methods

Sample preparation

Ice used in the experiment was pure polycrystalline, which consisted of columnar grains of a few centimeters in radius. An ice sphere (radius, $r_p = 1.5$ cm) as a projectile was formed from an ice cube (about $4 \times 4 \times 4\,\text{cm}^3$) by melting slowly between a pair of brass molds at a temperature of 15–25°C. The ice sphere was then taken out of the molds and stored in a cold room at −10°C.

The ice block as a target for higher temperature experiments (269–245 K) was $10 \times 10 \times 10\,\text{cm}^3$ in size and the mass ratio of the sphere to the block was about 0.01. The size of the ice block for lower temperature experiments (215–113 K) was $9 \times 9 \times 3.5\,\text{cm}^3$ (thickness = 3.5 cm) and the mass ratio was about 0.05. As these ice blocks were fixed firmly and their masses were much larger than the ice sphere (12 ± 1 g), the collision could be regarded as that between an ice sphere and an infinite mass body. The surface of ice blocks was prepared as smooth as possible by planing and polishing.

Temperature control

The temperature control of experiments was made by the following two methods. The experiments from 269 to 245 K were carried out in a large cold room, the temperature fluctuation of which was kept within 5°C. In the experiments from 215 to 113 K, a cryostat which was set in a large cold room (263 K) was used for the sample cooling (Fig. 2). The cooling method was similar to that developed by Arakawa and Maeno (1992). The sample temperature was controlled by regulating the flux of liquid nitrogen flowing into copper cooling platforms and could be regulated within 4°C in a vacuum condition. The regulation was realized by switching electronic valves with a micro-computer every 4 s. The cooling rates of copper cooling platforms were $\sim 4\,\text{K min}^{-1}$ for an ice sphere and $\sim 6\,\text{K min}^{-1}$ for an ice block. Temperatures were measured by use of copper–constantan thermocouples fixed on samples and cooling platforms.

The total time of one experiment was from ~30 min for 213 K to ~100 min for 113 K. The ambient space in this collision apparatus was evacuated with a rotary pump to the pressure of $\sim 10^3$ Pa which was low enough for thermal insulation but high enough so that sublimation and roughening the ice surfaces did not occur. The collision experiment was performed by pushing out the ice sphere with a drop bar attached to the top of the apparatus.

Measurements of restitution coefficient

Measurements of the restitution coefficient were performed by head-on collisions of an ice sphere freely falling on an ice block. The restitution coefficient of the ice sphere was defined as the ratio of the rebound velocity (v_r) to the impact velocity (v_i) of the ice sphere in the normal direction

$$\varepsilon = \frac{v_r}{v_i}. \tag{1}$$

The velocities of the ice sphere were measured by either a high speed video camera (200 or 500 frames s^{-1}) or acoustic emission (AE) signals. The latter method was similar to that used by Yen *et al.* (1970), which enabled us to calculate velocities accurately from time intervals between collisions. The AE sensor attached to the ice block surface could detect exact collision times and signals were monitored by a digital-oscilloscope. The impact velocity of the jth collision ($v_{i,j}$), where j is a number of collisions, is calculated from the time interval between $(j-1)$th and jth collisions (Δt_j, $j \geq 2$)

$$v_{i,j} = \frac{g\Delta t_j}{2} \tag{2}$$

where g is the acceleration due to gravity. The initial velocity ($v_{i,1}$) is calculated from the known height of the free fall (h)

$$v_{i,1} = \sqrt{2gh}. \tag{3}$$

Similarly the rebound velocity of the jth collision ($v_{r,j}$) was calculated as

$$v_{r,j} = \frac{g\Delta t_{j+1}}{2}. \tag{4}$$

When fracture occurred at the first collision, ε was measured for the largest fragment and subsequent ε data of $j > 2$ were not used.

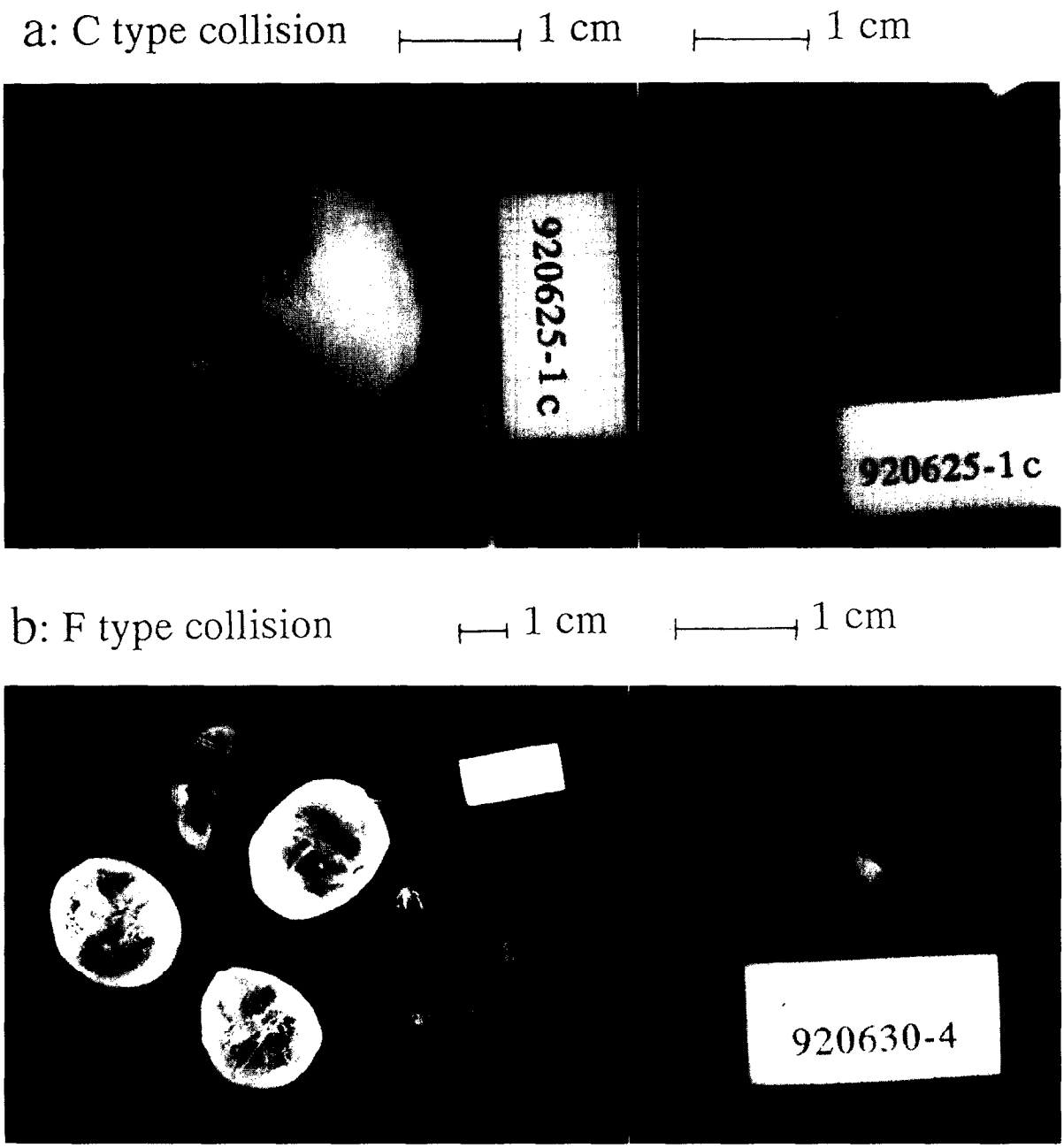

Fig. 3. Photographs of ice spheres (left) and ice block surfaces (right). (a) C type ($m_i/m_p = 0.99$, $T = 245\,\mathrm{K}$, $v_i = 150\,\mathrm{cm\,s^{-1}}$, $\varepsilon = 0.80$); (b) F type ($m_i/m_p = 0.50$, $T = 245\,\mathrm{K}$, $v_i = 260\,\mathrm{cm\,s^{-1}}$, $\varepsilon = 0.27$)

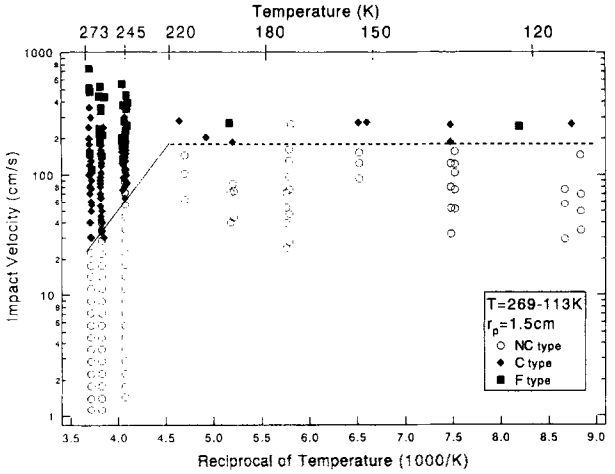

Fig. 4. Diagram to show the collision type of each experiment. Solid and dotted lines indicate a critical velocity between the quasi-elastic (NC type) and inelastic (C and F types) regimes

Experimental results

Types of collision

The collision behavior of ice spheres could be classified into three types: No-crack type (NC), Crack type (C) and Fragmentation type (F). In the NC type collision, no macroscopic fracture or deformation was observed at the impact point of the ice sphere and the ice block, but fracture patterns were observed in the C and F type collisions. At an intermediate velocity, many tiny cracks (white part in Fig. 3a) were formed around the impact point and small fragments were formed. As the impact velocity increased, vertical cracks appeared and grew to break the sphere into a few pieces (Fig. 3b). Figure 3a and b correspond to the C and F type collisions, respectively.

The C and F types were distinguished by the ratio of the largest fragment mass to the initial mass of the ice sphere (m_l/m_p). The ratio for the C type collision was defined as $0.95 \leq m_l/m_p \leq 1$. In this type, many cracks were formed around the impact point and produced small fragments. With the increase of the impact velocity vertical cracks were observed to grow from the impact point but the sphere did not break into pieces. In the F type collision the ratio was $m_l/m_p < 0.95$, and the ice sphere was broken into a few pieces by vertical crack planes. The degree of fracture of ice spheres and blocks increased with increasing v_i.

Figure 4 shows the collision types observed at various temperatures and impact velocities. When the temperature was kept constant, the collision types changed in the order of NC, C and F types with the increasing impact velocity. The critical velocity of fracture initiation increased with the decreasing temperature from 25 cm s^{-1} at $T = 269$ K to about 180 cm s^{-1} at $T = 215$ K, but was constant (180 cm s^{-1}) at lower temperatures (≤ 215 K).

Impact velocity dependence of restitution coefficient

Fig. 5a shows a typical result of restitution coefficients plotted against the impact velocity at $T = 261$ K. The velocity dependence of ε can be classified into two regimes by a critical velocity (v_c): the quasi-elastic regime ($v_i \leq v_c$) and inelastic regime ($v_i > v_c$).

In the quasi-elastic regime, ε is roughly constant. The average value is 0.90 ± 0.05, and the maximum values shown by the upper error bars are close to unity. The collision type is mostly NC type.

On the other hand, in the inelastic regime, ε decreased with increasing v_i and the collision type is C or F types, suggesting that the decrease of ε was caused by energy loss due to fracture. We tried to fit ε at $v_i > v_c$, by some

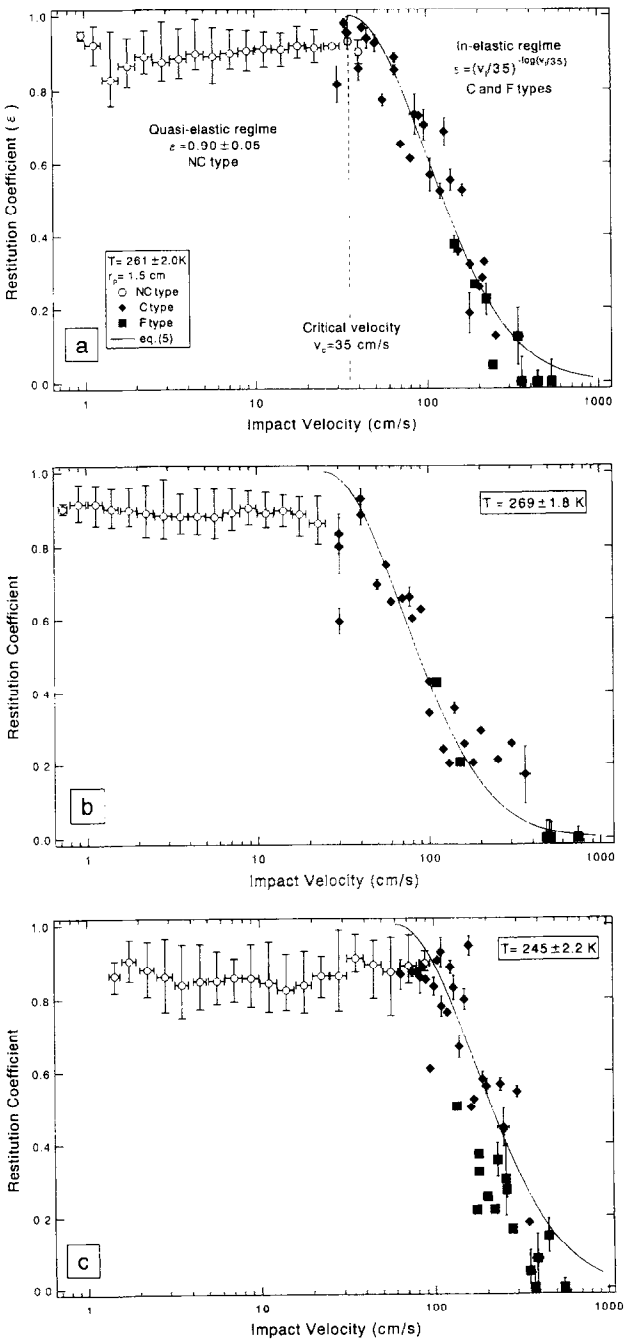

Fig. 5. Impact velocity dependence of ε. The curve for C type is equation (5). The open circle, the upper and lower error bars for NC type show the average, the maximum and the standard deviation, respectively. (a) $T = 261$ K; (b) $T = 269$ K; (c) $T = 245$ K

classical plastic deformation models based on the Hertzian theory such as Andrews', Tabor's and Johnson's models (see Dilley, 1993; Johnson, 1985), but none of these were satisfactory. Then we found the following empirical equation, which could fit the measured values of ε for C type collisions reasonably well

$$\varepsilon = \left(\frac{v_i}{v_c}\right)^{-\log(v_i/v_c)} \quad (5)$$

where v_c is a critical velocity ($v_c = 35\,\mathrm{cm\,s^{-1}}$ at 261 K, Fig. 5a) when ε equals to unity or no fractures take place. The ε data of F type lie below equation (5), because fragments are ejected radially from the impact point and carry away parts of the total kinetic energy. Equation (5) can be regarded as upper limits for F type collisions.

Hartmann (1978) made experiments on low-velocity impacts (1–50 m s^{-1}) with the purpose of broadly mapping the consequences of collisions of bodies in a wide range of relative speeds and sizes under the conditions of the primitive solar nebula. From collisions between centimeter-scale projectiles of different materials and a flat rock target, Hartmann determined a velocity which separated a shattering regime (defined by $m_l/m_p = 0.5$) from simple rebound. For ice projectiles, this velocity was 9 m s^{-1}. Since his experimental conditions (temperature and projectile size) have not been mentioned and he used a rock target, we could not compare his result with ours directly. However, in our experiments we never observed normal rebound at $m_l/m_p \sim 0.5$ because of the catastrophic fragmentation, so that $m_l/m_p = 0.5$ may be a reasonable separation criterion between the shattering regime and simple rebound.

Figure 5b and c show similar ε results at $T = 269$ and 245 K, respectively. The average values in the quasi-elastic regime are 0.89 ± 0.05 (269 K) and 0.86 ± 0.08 (245 K). This result implies the insignificant temperature dependence of the quasi-elastic restitution coefficient of ice. However, the value of v_c increased with decreasing T from 25 cm s^{-1} (269 K) to 61 cm s^{-1} (245 K).

Temperature dependence of restitution coefficient

Figure 6 gives ε as a function of the reciprocal of temperature ($1/T$). ε at lower impact velocities ($v_i = 140$–160 cm s^{-1}, Fig. 6a) increases rapidly with decreasing T and becomes a constant quasi-elastic value at temperatures below ~215 K. The collision type changes in the order of F, C and NC types with increasing ε. ε at higher impact velocities ($v_i = 250$–280 cm s^{-1}, Fig. 6b) also increases rapidly with decreasing T from 0.1 to 0.6 and becomes a constant inelastic value (about 0.6) at temperatures below 215 K. Although there was occasionally a high value of NC type collision, the collision type was mostly C or F type.

These temperature dependences give the following suggestions. First the temperature dependence above 215 K (Fig. 6a and b) suggests that v_c at these temperatures is smaller than 140 cm s^{-1} and increases with decreasing T. Second the constant quasi-elastic value at $T = 215$–113 K (Fig. 6a) implies that v_c is larger than 160 cm s^{-1}.

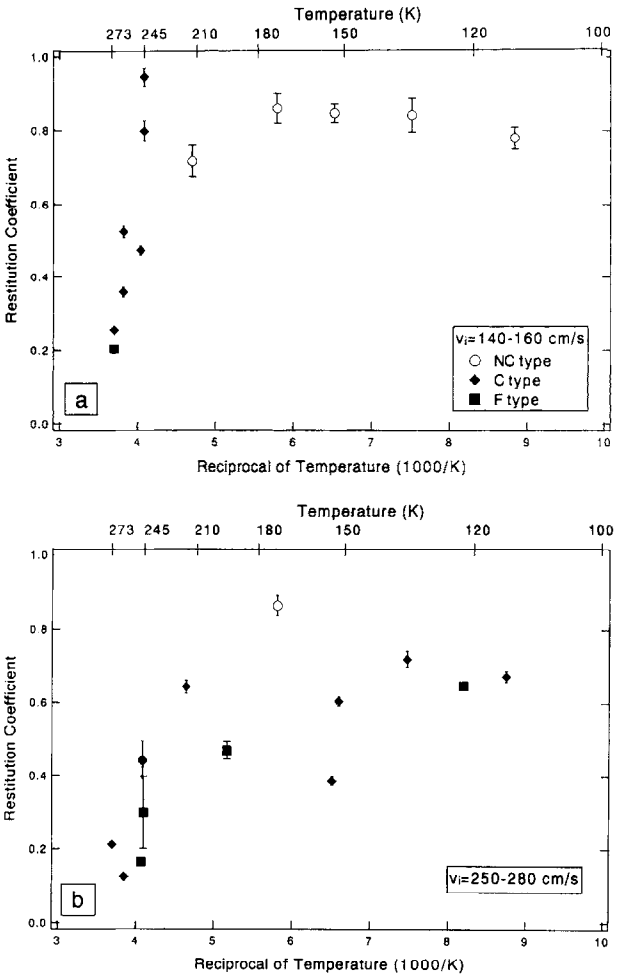

Fig. 6. Temperature dependence of ε. (a) $v_i = 140$–160 cm s^{-1}; (b) $v_i = 250$–280 cm s^{-1}

Finally the constant inelastic value at $T = 215$–113 K (Fig. 6b) suggests that v_c is constant irrespective of T and smaller than 250 cm s^{-1}.

Effects of frost

Figure 7 shows examples of the impact velocity dependence measured at two lower temperatures $T = 215$–173

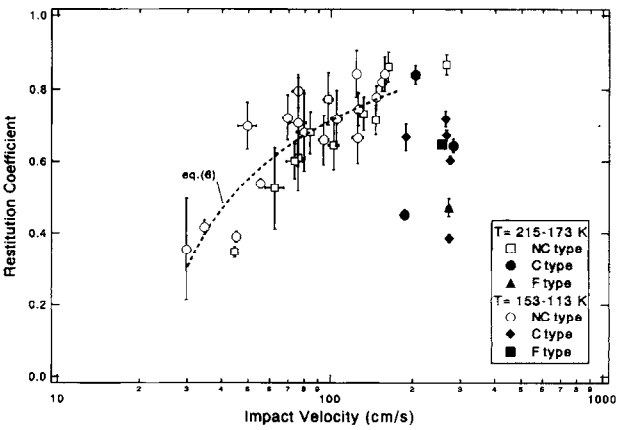

Fig. 7. Impact velocity dependence of ε at temperatures 215–113 K for frosted ice

and 153–113 K. As we see the temperature dependence is insignificant. With the increase of v_i, ε increases from 0.3 to 0.8 and decreases rapidly at larger velocities than 180 cm s^{-1}. The behavior of ε at lower velocities than 180 cm s^{-1} was caused by thin frost layers on the ice surfaces. As expected from Fig. 5, this velocity region is the quasi-elastic regime if the ice sphere and the ice block are frost free. As the fracture strength of frost is weaker than that of ice, frost is deformed by the collision even if v_i is lower than v_c of the frost-free ice sphere. Since the frost layer thickness is finite, the energy dissipation by the deformation can be negligibly small compared to the initial kinetic energy depending on their relative magnitudes. As a result, ε of a frosted sphere increases with increasing v_i until the velocity of ice fracturing (180 cm s^{-1}) is reached. The value, $\varepsilon = 0.86$ at 160 cm s^{-1}, is comparable to the typical value in the quasi-elastic regime at higher temperatures (269–245 K). Surface conditions are important for energy loss at lower impact velocities, but this effect becomes negligible with increasing v_i.

The observed data of ε with effects of frost deformation were fitted as follows. If the energy loss (E_{loss}) due to the frost deformation can be expressed by the product of a deformation volume of the frost layer (ΔV) and the power of the impact velocity (v_i^p), concerning the conservation of energy, we can write ε as

$$\varepsilon = \sqrt{\frac{\frac{1}{2}m_p v_i^2 - E_{loss}}{\frac{1}{2}m_p v_i^2}} = \sqrt{1 - \frac{2c_1 \Delta V v_i^{p-2}}{m_p}}$$

where c_1 and p are constants. As ΔV is constant due to the finite thickness of the frost layer, we get

$$\varepsilon = \sqrt{1 - \frac{c_2 v_i^{p-2}}{m_p}} \qquad (6)$$

where c_2 is constant. This equation could fit all the data of NC type at $T = 215$–113 K, $\varepsilon = \sqrt{1 - 5.3 v_i^{-0.52}}$ (Fig. 7).

The decrease of ε at higher velocities than 180 cm s^{-1} is caused by the fracture of ice, suggesting that the region corresponds to the inelastic regime. Though v_c could not be specified from equation (5) due to insufficient data, it could be estimated as about 180 cm s^{-1} (215–113 K) based on the experiments at higher temperatures (269–245 K). In the lower temperature range, v_c will show no temperature dependence. The result is different from that in the higher temperature range (269–245 K).

Table 1 summarizes the temperature dependence of ε and v_c for smooth frost-free surfaces. The value of ε in the quasi-elastic regime was calculated as the average values of NC type collisions.

Table 1. Restitution coefficient in the quasi-elastic regime and critical velocity

Temperature (K)	ε in the quasi-elastic regime	v_c (cm s^{-1})
269 ± 1.8	0.89 ± 0.05	25
261 ± 2.0	0.90 ± 0.05	35
245 ± 2.2	0.86 ± 0.08	61
215–113	0.87 ± 0.031[a]	180[b]
	Average = 0.88	

[a] The maximum value measured in NC type.
[b] Estimated from the onset of ice fracturing.

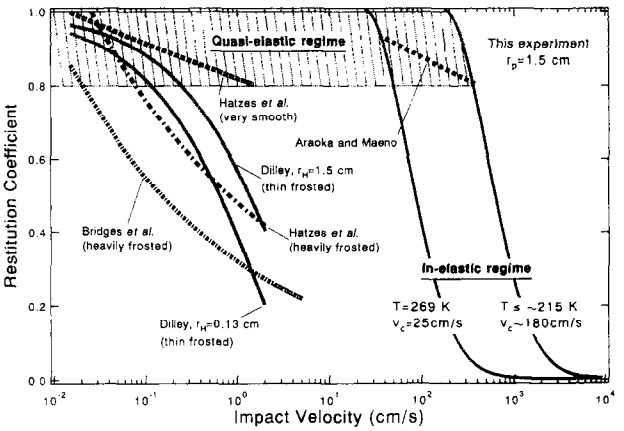

Fig. 8. Various results of restitution coefficients of ice. The shaded area indicates the quasi-elastic regime. The empirical equation ($\varepsilon = 1.71 v_i^{-0.063}$) of Araoka and Maeno (1978) data is given in Maeno (1991)

Discussion and conclusions

Figure 8 is the summary of our results together with those of previous works which were made to determine ε of ice spheres in collisions between an ice sphere and an ice block, and Table 2 summarizes the experimental conditions.

First, we discuss the case of frost-free surfaces, and compare our results with those of Araoka and Maeno (1978) and the "very smooth" ice spheres of Hatzes *et al.* (1988). Hatzes *et al.* measured the restitution coefficient of ice spheres with respect to the surface characteristics and the radius of curvature of ice samples, and concluded that ε of the "very smooth" ice is independent of the radius of curvature. We can point out that although both Araoka and Maeno and Hatzes *et al.* show weak velocity dependencies, their ε values are within 0.8–1 and included in our quasi-elastic regime (hatched region in Fig. 8). This implies that ε is roughly constant (0.8–1) irrespective of r_p (either the radius or the radius of curvature), v_i and T. If we compare ε of Araoka and Maeno with ours at the same temperature (261 K), we note that the quasi-elastic regime for Araoka and Maeno ($r_p = 0.13$ cm) extends to higher velocities than $v_c = 35$ cm s^{-1} ($r_p = 1.5$ cm, $T = 261$ K). This size dependence indicates that v_c increases with decreasing r_p and that fracture becomes harder to occur with decreasing r_p. If we recall that ice particles in Saturn's main rings have size distributions ranging from 1 cm to 5 m radius (Marouf *et al.*, 1983), we must say that experiments on the size dependence of ice particle collision are very important.

Hatzes *et al.* (1988) investigated the radius of curvature dependence of ε for ice spheres with a thin layer of compacted frost on the surface ("thin frosted") and showed

Table 2. Experimental conditions

Authors	Ice sphere/block surface conditions	Radius (cm)	Impact velocity ($cm\,s^{-1}$)	Temperature (K)	Method
Araoka and Maeno (1978)	frost-free	0.13	40–400	261	free fall
Bridges *et al.* (1984)	heavily frosted	2.75	0.015–5.1	150–175	disc pendulum
Hatzes *et al.* (1988)	very smooth	2.5, 10[a]	0.015–2	105	disc pendulum
	thin frosted	2.5, 5,[a] 10,[a] 20[a]	0.015–2	123–133	disc pendulum
	heavily frosted	2.5	0.015–2	123	disc pendulum
Supulver *et al.* (1995)	frost-free	2.5	0.02–1	100	disc pendulum
Present study	frost-free	1.5	1–700	245–269	free fall
	frosted	1.5	30–280	113–215	free fall

[a]The radius of curvature at the impact point.

that ε increased with the increasing radius of curvature (r_H). Using a viscous dissipation model (Dilley, 1993), Dilley fitted the Hatzes *et al.* data by $\varepsilon = \exp(-\pi\xi/\sqrt{1-\xi^2})$ where $\xi = 0.16(r_H/2.5\,\mathrm{cm})^{-0.2}v_i^{0.65}$. Figure 8 shows the calculated value of ε at $r_H = 0.13$ and 1.5 cm; ε decreases with the decreasing r_H. Although Dilley suggested that the radius of curvature dependence may not be the true size dependence in the case of actual sphere collisions, his model predicts that ε decreases with the decreasing radius. This predicted size dependence is opposite to that obtained by the comparison of our data and that of Araoka and Maeno. To get more definite size dependence, further experiments are needed on different sizes of ice spheres (both smooth and frosted).

Next, we discuss the velocity dependence of frosted surfaces, and compare our results with the "thin frosted" ice spheres of Hatzes *et al.* (1988) and the more heavily frost covered ice sphere ("heavily frosted") of Bridges *et al.* (1984). Hatzes *et al.* (1988) confirmed by experiments that ε of ice with frost was smaller than that without frost and the velocity dependence was related to surface characteristics (thin/heavily frosted). Their results with frost showed that ε decreased with increasing v_i in contrast with our results shown in Fig. 7.

As mentioned above, these "thin frosted" ice data by Hatzes *et al.* (1988) were fitted by Dilley's model. Dilley showed that ε could not be fitted by classical plastic deformation models and developed the viscous dissipation model by treating the "thin frosted" ice surfaces as a Kelvin–Voigt solid. His model indicated that the decrease of ε is caused by energy dissipation within surface frosts, the degree of which increases with increasing v_i.

Recently a theoretical model of the restitution coefficient for elastic–plastic material was derived by Johnson (1985) who showed that ε decreased with increasing v_i in a form $v_i^{-1/4}$ when the velocity was large enough to cause plastic deformation. This velocity dependence could explain the experimental results of various materials compiled by Goldsmith (1960). The data of Bridges *et al.* could be fitted by $\varepsilon = 0.32v_i^{-0.234}$, and its power index is very close to $-\frac{1}{4}$. Similarly for the "heavily frosted" ice of Hatzes *et al.* (1988), $\varepsilon = 0.48v_i^{-0.20}$ and its power index is close to $-\frac{1}{4}$ again. We may assume that the decrease of ε is caused by frost deformation. It is clear that the opposite velocity dependence of ε shown in Fig. 7 cannot be explained by these models. As already stated, it is necessary to take into account the finite deformation of the frost layer.

When the ice particles are frosted, the size/velocity dependence of ε is complex. Hartmann (1978) discussed how the presence of the regolith layer of planetesimals affects the planetary growth. In his collision experiments between smooth basalt spheres (0.13–5.0 g) and smooth rock target covered with rock powder, the restitution coefficient rapidly decreased with the increasing ratio of regolith depth to projectile diameter at a constant velocity (1.4–$6.2\,m\,s^{-1}$). The effect of this regolith layer on ε is considered similar to that of the frosted ice surfaces. His results may be applied to future investigation of ε for frosted surfaces. In future experiments of the impact velocity dependence of ε for frosted surfaces, we should systematically vary sphere size and control the ratio of frost depth to projectile diameter.

Finally on the basis of the above discussion, the restitution coefficient of smooth frost-free ice at Saturn's temperature condition $\simeq 100$ K should be described by the experimental results of the "very smooth" ice of Hatzes *et al.* (1988) when v_i is less than $\sim 1\,cm\,s^{-1}$, and our results at larger than $\sim 1\,cm\,s^{-1}$

$$\varepsilon = \begin{cases} 0.82v_i^{-0.047} & v_i \leq \sim 1\,\mathrm{cm\,s^{-1}} \\ \sim 0.88 & \sim 1\,\mathrm{cm\,s^{-1}} < v_i \leq v_c \\ \left(\dfrac{v_i}{180}\right)^{-\log(v_i/180)} & v_c < v_i \end{cases} \quad (7)$$

When the ring particles are smooth, frost-free ice spheres, calculations of the orbital evolution of particles should be done using equation (7). This high value of ε at $T \simeq 100$ K is inconsistent with the present thin Saturn rings whose upper limit is less than 100–200 m set by *Voyager* measurements (Lane *et al.*, 1982). A value of $\varepsilon > 0.9$ for collision velocities up to $180\,cm\,s^{-1}$ could yield a ring thickness greater than a kilometer (Goldreich and Tremaine, 1978). Thus ice particles in the present Saturn rings cannot be smooth, frost-free surfaces. However, even if particles surfaces were initially smooth frost-free, they might be thin frosted as a consequence of collision cracks and fragmentations at higher impact velocities due to the increasing velocity dispersion.

In order to simulate ice particles in Saturn's rings, we also need to study the restitution coefficient at glancing

collisions. According to Supulver *et al.* (1995), who used the "frost-free" ice sphere, the restitution coefficient in the tangential collision gave higher values and could be fitted by $\varepsilon = 0.88 - 0.0038 v_t$, where v_t is the velocity in the tangential direction. The complex dependence of the restitution coefficient of ice on temperature, velocity, frost layer, possibly size and collision angle should be taken into account in elucidating the formation process of Saturn's rings, and more experimental data are needed to determine those dependences.

Acknowledgements. We acknowledge greatly the technical help of T. Segawa and S. Nakatsubo of the Construction Division of Inst. Low Temp. Sci., Hokkaido University. We also acknowledge Dr K. Ohtsuki of Yamagata University for useful suggestions, and Drs H. Narita, K. Nishimura, K. Kosugi and others of Inst. Low Temp. Sci., Hokkaido University for encouragement. We acknowledge Dr J. Dilley of Ohio University and Dr J. Blum of Max-Planck Institute for their useful advice to improve our manuscript.

References

Arakawa, M. and Maeno, N., Mechanical deformation of polycrystalline ice I_h at temperature 100–263 K : First Report, in *Physics and Chemistry of Ice* (edited by N. Maeno and T. Hondoh), pp. 464–469. Univ. of Hokkaido Press, Sapporo, 1992.

Araoka, K. and Maeno, N., Measurements of restitution coefficients of ice. *Low Temp. Sci., Ser. A* **36,** 55–65, 1978 (in Japanese with English summary).

Bridges, F. G., Hatzes, A. P. and Lin, D. N. C., Structure, stability and evolution of Saturn's rings. *Nature* **309,** 333–335, 1984.

Dilley, J. P., Energy loss in collisions of icy spheres : loss mechanism and size–mass dependence. *Icarus* **105,** 225–234, 1993.

Esposito, L. W., Structure and evolution of Saturn's rings. *Icarus* **37,** 345–357, 1986.

Goldreich, P. and Tremaine, S., The velocity dispersion in Saturn's rings. *Icarus* **34,** 227–239, 1978.

Goldsmith, W., *Impact.* Arnold, London, 1960.

Greenberg, R., Davise, D. R., Hartmann, W. K. and Chapman, C. R., Size distribution of particles in planetary rings. *Icarus* **30,** 769–779, 1977.

Hartmann, W. K., Planet formation : mechanism of early growth. *Icarus* **33,** 50–61, 1978.

Hatzes, A. P., Bridges, F. G. and Lin, D. N. C., Collisional properties of ice spheres at low impact velocities. *Mon. Not. R. Astron. Soc.* **231,** 1091–1115, 1988.

Higa, M., Arakawa, M. and Maeno, N., Impact experiment of ice spheres on an ice block : First Report. *Proc. 26th ISAS Lunar and Planetary Symp.*, pp. 141–144, 1993.

Johnson, K. L., *Contact Mechanics*, pp. 340–373. Cambridge Univ. Press, London, 1985.

Lane, A. L., Hord, C. W., West, R. A., Esposito, L. W., Coffeen, D. L., Sato, M., Simmons, K. E., Pomphrey, R. B. and Morris, R. B., Photopolarimetry from Voyager 2 : preliminary results on Saturn, Titan and the rings. *Science* **215,** 537–543, 1982.

Maeno, N., Physical properties of snow and ice particles. *J. Geography* **100**(2), 224–233, 1991 (in Japanese with English summary).

Marouf, E. A., Tyler, G. L., Zebker, H. A., Simpson, R. A. and Eshleman, V. R., Particle size distributions in Saturn's rings from Voyager I radio occultation. *Icarus* **54,** 189–211, 1983.

Ohtsuki, K., Equilibrium velocities in planetary rings with low optical depth. *Icarus* **95,** 265–282, 1992.

Supulver, K. D., Bridges, F. G. and Lin, D. N. C., The coefficient of restitution of ice particles in glancing collisions : experimental results for unfrosted surfaces. *Icarus* **113,** 188–199, 1995.

Yen, Y. C., Odar, R., Asce, A. M. and Bracy, L. R., Impact of spheres on ice. *Proc. Am. Soc. Civil Engrs J. Engng Mech. Div.* **EM5,** 641–652, 1970.